

## EDDY CURRENT DETECTION OF NUCLEATION AND EARLY GROWTH OF SEMICONDUCTOR CRYSTALS

Bill W. Choi, Kumar P. Dharmasena and Haydn N.G. Wadley  
Intelligent Processing of Materials Laboratory  
School of Engineering and Applied Science  
University of Virginia  
Charlottesville, VA 22903

### INTRODUCTION

Single crystal CdTe and its solid solution  $\text{Cd}_{1-x}\text{Zn}_x\text{Te}$  alloys ( $0.03 < x < 0.05$ ) are used as infrared transparent substrates for infrared focal plane array (IRFPA) detectors[1,2].  $\text{Cd}_{1-x}\text{Zn}_x\text{Te}$  substrates are normally “mined” from large polycrystalline boules grown by the unseeded directional solidification of  $\text{Cd}_{1-x}\text{Zn}_x\text{Te}$  melts using either a vertical or horizontal Bridgman process[3-7]. The vertical Bridgman method is particularly popular for growing CdTe and its related compounds. In this process, a  $\text{Cd}_{1-x}\text{Zn}_x\text{Te}$  ingot is produced by first melting a charge in the hot zone of the furnace and then vertically translating the furnace (with its associated axial temperature profile) relative to the stationary crucible to cause directional solidification. In spite of many experimental efforts to investigate the relationships between material purity, stoichiometry, the growth parameters (furnace temperature profiles, ampoule geometries/materials, furnace translation rates and starting position) and the resulting material characteristics (grain structure, dislocation densities, IR transmission, macro-segregation etc.), the yield of  $\text{Cd}_{1-x}\text{Zn}_x\text{Te}$  of a quality suitable for large area (e.g. 4cm x 6cm) substrates remains low (<10%). Since much of this poor yield is directly associated with the crystal growth process (e.g. melt stoichiometry, solidification velocity, interface shape, temperature gradients, cooling rate, etc.) intensive efforts are under way to improve this technology.

The large difference in the electrical conductivity of the solid and liquid phases of  $\text{Cd}_{1-x}\text{Zn}_x\text{Te}$  at its melting point suggests eddy current sensing methods for monitoring crystal growth[8-11]. The basic principle underlying the application of eddy current techniques to semiconductor crystal growth is the detection of perturbations to the electromagnetic field created by an a.c. excited solenoid arising from induced (eddy) currents in the test sample. The intensity of these eddy currents depends on the electrical conductivity distribution within the sample (i.e. the conductivity of the liquid and solid phases and the position of a liquid-solid interface), the distribution of electromagnetic flux within the test material (governed by the sensor/test material geometry and excitation frequency) and the rate of change of the electromagnetic flux (i.e. the test frequency). If the perturbations associated with solidification processes can be measured and analyzed, it may

be possible to non-invasively obtain new information about the growth process. Earlier work used an eddy current sensor positioned in the cylindrical region of the vertical Bridgman growth ampoule to enable the characterization of the liquid-solid interface about midway through a growth process[10,11]. Here, we focus on the use of a sensor positioned to interrogate the first to freeze region of the ingot. The results provide new insights about solid nucleation and the early stage of solidification in this crystal growth system, and provide new opportunities to control nucleation and growth.

## FINITE ELEMENT SIMULATIONS

An electromagnetic finite element model was used to relate the multifrequency transfer impedance response of a two coil eddy current sensor to the movement of a  $\text{Cd}_{0.955}\text{Zn}_{0.045}\text{Te}$  liquid-solid interface located within a pyrolytic boron nitride (PBN) crucible with a conically shaped end. The geometry was axisymmetric and therefore required only a two-dimensional analysis. The finite element model inputs were the sample shape, sensor geometry, input current to the driver coil, test frequency, liquid-solid interface location, and the electrical conductivities of the solid and melt. The model output was the magnetic vector potential from which the induced voltage in a pickup coil region and the sensor's complex transfer impedance could be calculated. Details of the procedures have been reported elsewhere[12].

The initial set of calculations used a liquid conductivity value (6550 S/m) for the sample. A second set used a value of 1400 S/m representative of the solid. Additional sets of calculations were conducted with a flat boundary separating regions of liquid and solid that could be incrementally advanced through the cone area to simulate solid nucleation and subsequent crystal growth. Due to the decrease in electrical conductivity during solidification of most semiconductors, the imaginary impedance component monotonically increases with time (i.e. the extent of solidification during the crystal growth process). Fig. 1 shows the variation of the normalized imaginary component of the cone sensor's impedance at test frequencies of 50kHz, 200kHz, 500kHz, and 1.2MHz as a function of interface location measured from the cone tip. In the initial stages (a complete melt condition), the imaginary impedance has a value corresponding to the liquid's electrical conductivity. During the propagation of a liquid-solid interface in the cone region of the ampoule, the interface position,  $h$ , changes from zero (in the cone tip) to 45mm (at the cone-cylinder shoulder) and the impedance increases at all frequencies. When a liquid-solid interface has propagated sufficiently far from the tip of the ampoule (>45mm), the imaginary impedances at each test frequency asymptotically converge to values corresponding to the solid's electrical conductivity.

At frequencies less than 200kHz, the rate of change of electromagnetic flux within the cone region is sufficiently weak that eddy current induction barely occurs, the sample appears to be electromagnetically transparent, and the resulting impedance change is small (close to the null response of the sensor). At high test frequencies (>1MHz), the increased rate of change of flux induces intense eddy currents and results in a larger change in the initial response to the liquid-solid interface up to a distance of about 25mm. At larger distances, the response is weakened due to rapid spatial decay of the high frequency induction field of the sensor. A more continuous impedance increase is observed over a larger distance at 500kHz where both the eddy current density and the "sensed" sample volume are large. This frequency appears to be the best suited for analyzing nucleation and growth within the ampoule tip.

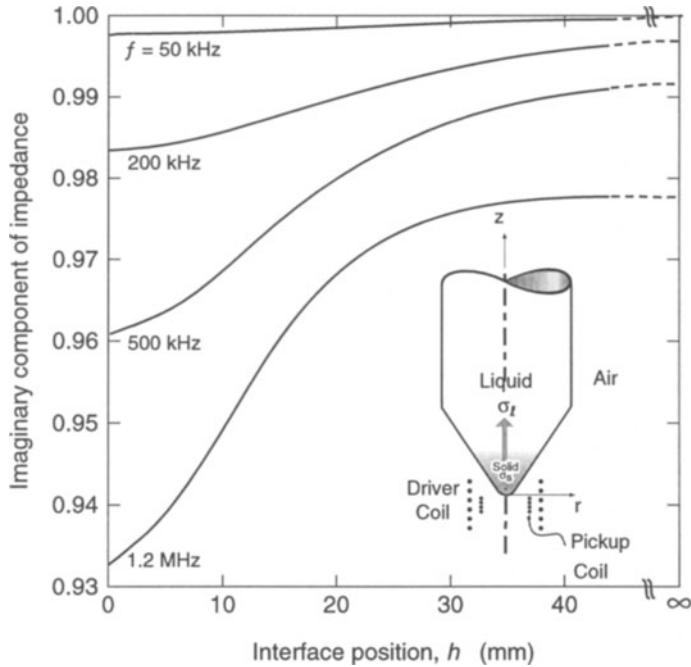


Figure 1. Calculated imaginary impedance variation for a two coil eddy current sensor with interface position,  $h$  (measured from the ampoule tip), at four test frequencies. A six turn driver coil is used to excite an electromagnetic field and a four turn pickup coil detects the perturbation of the primary coil's field resulting from the presence of the conducting sample.

## EXPERIMENTAL PROCEDURES

### Sensor Design and Measurement Methodology

A two-coil eddy current sensor with a design similar to that analyzed by the finite element model was constructed and installed in a commercial scale 17-zone vertical Bridgman furnace. To eliminate disturbances to the thermal environment, the sensor was integrated into the pre-existing concentric alumina tubes used to support the sample containing quartz ampoule (Fig. 2). The driver (primary) and pickup (secondary) coils were wound within grooves machined on the outer surfaces of the two smallest tubes. The primary coil consisted of 6 turns of 18AWG platinum wire wound over a length of 38.1mm. The secondary coil had 4 turns of 30AWG platinum wire wound over a 12.7mm length.

A schematic circuit diagram of the measurement system is shown in Fig. 3. A continuous signal to the primary coil was supplied by the variable frequency oscillator within a Hewlett Packard (HP4194A) Impedance Gain/Phase Analyzer. This signal was amplified with a Model 25A100 (Amplifier Research Inc.) amplifier to enhance the field strength of the primary coil. Frequency dependent gain measurements ( $G$ ) for the two coil system were obtained by recording the ratios of the voltage induced across the secondary coil with the voltage drop across a 1 ohm low inductance precision resistor in the primary circuit. The phase difference ( $\phi$ ) between these two voltage signals was also monitored. Gain and phase measurements were first recorded for the empty sensor ( $G_0, \phi_0$ ) at the high

temperatures normally used for  $\text{Cd}_{0.955}\text{Zn}_{0.045}\text{Te}$  crystal growth. Measurements were repeated at 10 minute intervals during crystal growth and normalized with respect to the empty sensor measurements to emphasize the effect of the growing crystal.

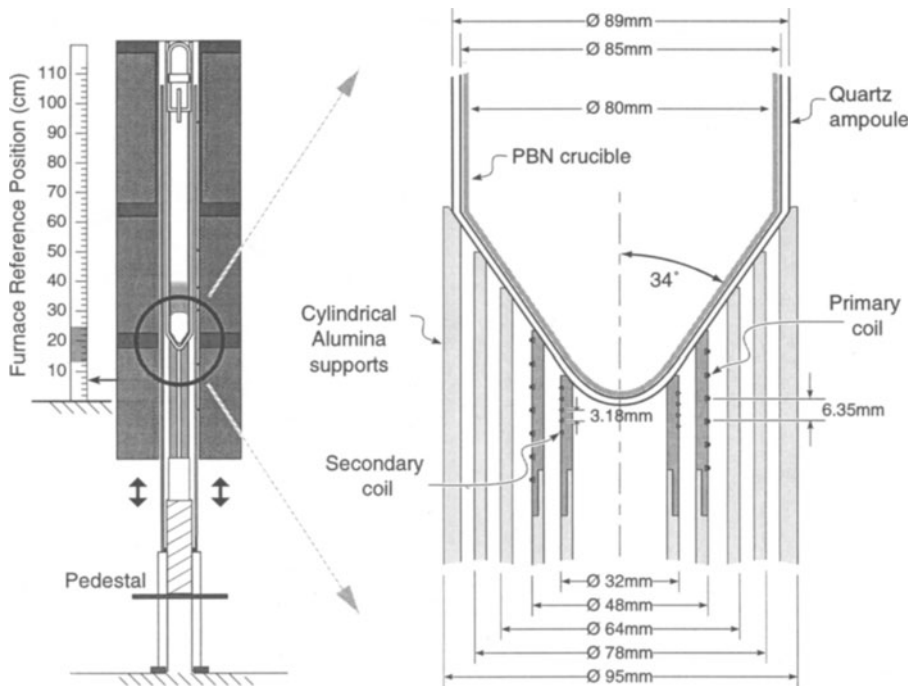


Figure 2. Schematic diagram of the eddy current sensor installed near the ampoule tip of a 17-zone production scale vertical Bridgman furnace.

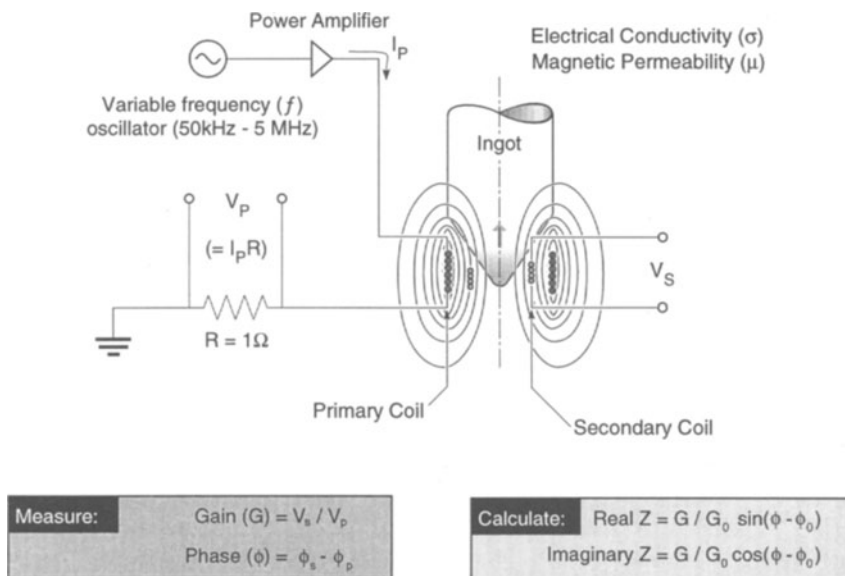


Figure 3. A schematic circuit diagram of the two-coil impedance measurement system using a HP 4194A Impedance/Gain-Phase analyzer.

## Growth Experiments

A series of three  $\text{Cd}_{0.955}\text{Zn}_{0.045}\text{Te}$  crystal growth experiments (CZT0322, CZT0328, and CZT0405) were monitored with the eddy current sensor using the same charge. The 3.3kg charge consisting of Cd, Zn and Te and pieces of precompounded CdTe were placed in a 80mm diameter pyrolytic boron nitride (PBN) crucible for run CZT0322. The PBN crucible was contained within a 85mm diameter sealed quartz ampoule. The furnace was lowered to a start position of 7.4cm on a reference scale (Fig. 2) to expose the in-situ compounding charge to the high temperatures needed to achieve complete mixing. Run CZT0328 was performed by re-melting the solidified ingot from CZT0322 at a furnace start position of 9.3cm. The starting sample configuration and the furnace start position were the same for experiments CZT0328 and CZT0405.

Schedules for each run consisted of several time segments for heating, furnace movement (translation or hold) and cooling. These were programmed and executed through a personal computer based process controller. Segments 1-3 covered the period during which the furnace temperature was gradually increased to 1153°C. For runs CZT0328 and CZT0405, a longer time was programmed in segment 3 to allow complete melting of the precompounded  $\text{Cd}_{0.955}\text{Zn}_{0.045}\text{Te}$  ingot formed after runs CZT0322 and CZT0328 respectively. Upon reaching the maximum temperature, a soak of 10 hours was used to allow the melt to reach equilibrium before initiating movement of the furnace. Segment 5 in CZT0322 (which raised the furnace at 1.87mm/hr over a 10 hour period) was included for the furnace to be brought from its start position of 7.4cm to 9.3cm before proceeding with movement at a slower rate of 1.49mm/hr similar to CZT0328/CZT0405. An interrupted growth strategy of a furnace translation segment followed by a furnace hold segment was adopted with the intention of inducing nucleation to occur within the conically shaped region of the ampoule.

## RESULTS

### Compounding/Melting Stage

Fig. 4 shows a comparison of the high temperature normalized imaginary impedance response and the estimated cone tip temperature as a function of time for experiments CZT0322 and CZT0405. Results of experiment CZT0328 were very similar to those shown for CZT0405 (and are not shown) since both experiments were performed under the same conditions. Within the first 1.1 hours of heating, the furnace had reached 700°C by which time the elemental Cd, Zn and Te had melted in CZT0322 (Fig. 4a) causing the impedance to initially decrease, before increasing sharply when the elements reacted to form the lower conductivity  $\text{Cd}_{0.955}\text{Zn}_{0.045}\text{Te}$  compound. This phenomena was not observed in CZT0405 (Fig. 4b), since no elemental material was present and the electrical conductivity of solid  $\text{Cd}_{0.955}\text{Zn}_{0.045}\text{Te}$  (the starting ingot) is much lower requiring higher temperatures to cause a significant impedance change to occur at any of the frequencies. At the beginning of segment 4, a furnace set point temperature of 1153°C was reached. From the temperature profile and the starting position of the furnace (7.4cm for CZT0322 and 9.3cm for CZT0405), the cone tip temperatures were estimated to be around 1092°C and 1080°C respectively.

For CZT0322, it took approximately 2 hours of the 10 hour soak period (segment 4) for the charge to completely melt (to the bottom of the cone tip) and the frequency dependent impedance values to stabilize. A comparison of the experimental impedance

value at 500kHz (0.962) with the finite element calculation in Fig.1(0.961 at  $h=0$  representing the liquid state) confirms the existence of a complete melt. In contrast, in CZT0405 with a higher start position (i.e. lower cone tip temperature of 1080°C) melting occurred more slowly and did not appear to have reached a quiescent state at the end of segment 4. Indeed, the impedance value of 0.970 (at 500kHz) for CZT0405 indicates the presence of some solid at the cone tip. Using the simulated impedance response vs. interface position curve at 500kHz (Fig. 1), the starting ingot for Run CZT0405 was found to have slowly melted to within ~10mm from the ampoule tip (Fig.5).

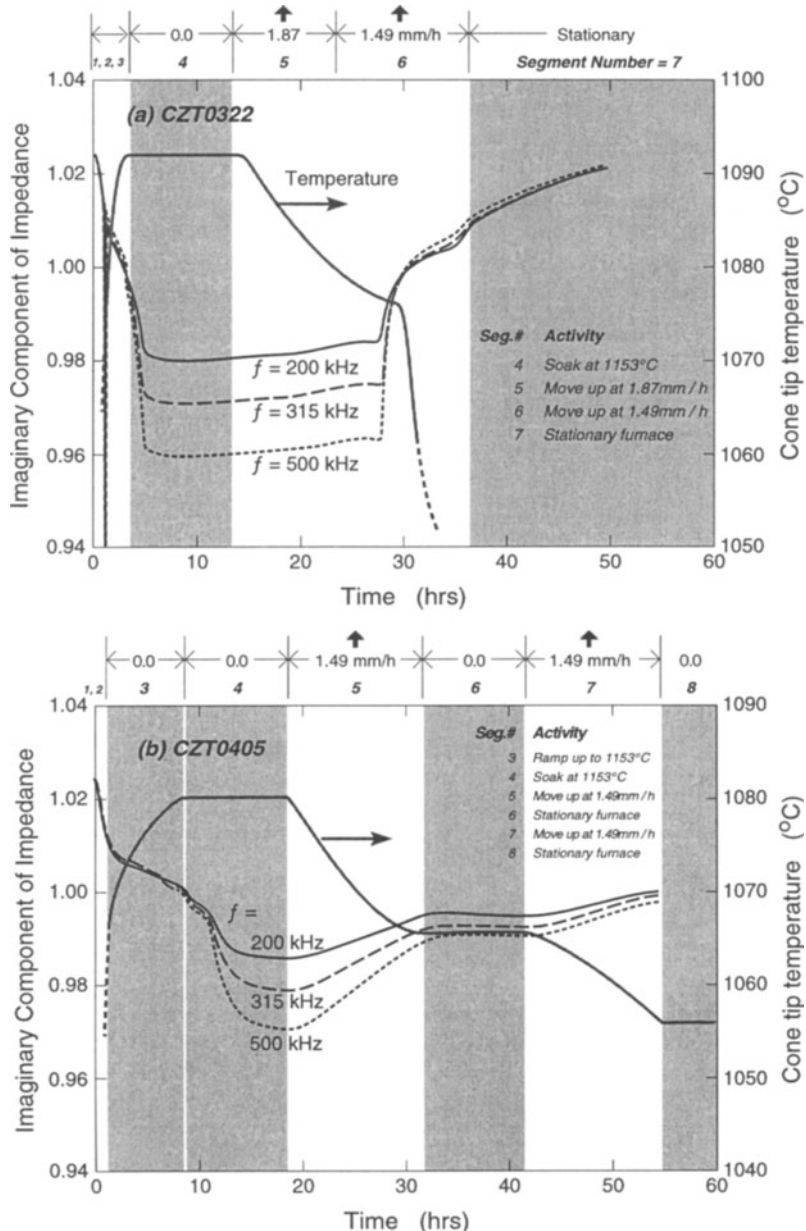


Figure 4. Measured impedance response at three frequencies and the estimated cone tip temperature during initial melting/compounding and subsequent nucleation/growth of  $\text{Cd}_{0.955}\text{Zn}_{0.045}\text{Te}$ . (a) CZT0322 (b) CZT0405.

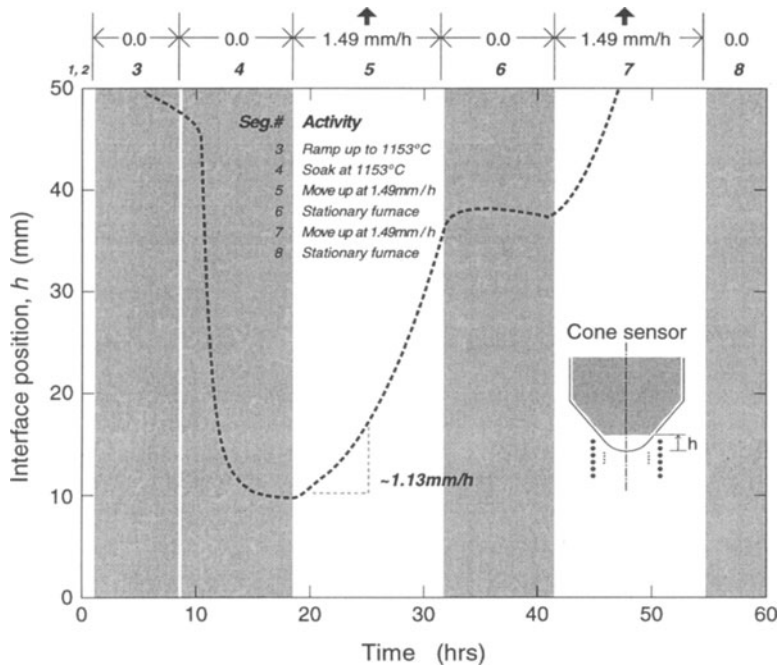


Figure 5. The solid-liquid interface movement during the melting and initial stages of growth for Run CZT0405. Incomplete melting is clearly observed with a ~10mm solid region remaining in the ampoule tip, after which the interface is seen to move at 1.13mm/h.

### Solid Nucleation and Initial Growth

An additional segment (#5) was included in CZT0322 to raise the furnace from its 7.4cm start position to reach 9.3cm at a translation rate of 1.87mm/hr before commencing the interrupted growth strategy of translation-hold-translation, Fig. 4a. During this 10 hour period, eddy current data did not change and so the molten state was maintained even though the temperature of the cone tip decreased by 12°C to 1080°C (a 18°C supercooling). The furnace was translated at a slower rate of 1.49mm/hr in segment 6 and further supercooling occurred. At 4.8 hours into this segment (~27.8 hours of processing time and a 20°C supercooling) a rapid increase in impedance was observed for all frequencies followed by a convergence to a single curve indicating the detection of a solid phase in the vicinity of the sensor and a detection of the moment of nucleation. Having determined the moment of nucleation, it is possible to use the result from the finite element analysis (Fig. 1) to determine the initial interfacial location as a function of time by comparison of the imaginary component values at 500kHz. The unstable solidification event caused the interface position to move upwards about 19mm from the cone tip in a 20 minute period (2 data collection cycles). The solidification rate during the nucleation period was found to be 57mm/h compared to a furnace translation rate of 1.49mm/h.

In contrast, impedance data collected during the corresponding furnace translation (at 1.49mm/hr) for the CZT0405 run does not show any rapid increase. What is observed is a more gradual increase in impedance indicating the upward movement of the liquid-solid interface which existed at the end of segment 4 due to incomplete melting. Using the finite element simulation of the interface movement in Fig. 1, the experimental impedance changes

was used to determine the local growth velocity. Fig.5 clearly shows that complete melting never occurred and a liquid-solid interface existed at the beginning of the furnace translation and advanced initially at 1.13mm/h.

## SUMMARY

Electromagnetic finite element analysis has been used to design an eddy current sensor for detecting and characterizing the nucleation of solid  $\text{Cd}_{1-x}\text{Zn}_x\text{Te}$  during vertical Bridgman growth. By using existing structures in a commercial scale furnace to support the sensor coils, an almost completely non-invasive sensor has been constructed and used monitor early stage solidification of 80mm  $\text{Cd}_{0.955}\text{Zn}_{0.045}\text{Te}$  ingots. When a fully melted charge was cooled, a 20°C supercooling was detected and a high velocity (~57mm/h) solidification front propagated about 20mm up the ampoule. The cooling of incompletely re-melted samples failed to cause supercooling or unstable growth. This sensor method creates new possibilities for feedback control of the re-melting and solidification process that could enable the reliable use of seeded growth strategies.

## ACKNOWLEDGMENTS

This work has been performed as a part of the research of the Infrared Materials Producibility Program conducted by a consortium that includes Johnson Matthey Electronics, Texas Instruments, II-VI Inc., Loral, the University of Minnesota, and the University of Virginia. We are grateful for the many helpful discussions with our colleagues in these organizations. The consortium work has been supported by ARPA/CMO under contract MDA972-91-C-0046 monitored by Raymond Balcerak.

## REFERENCES

1. W.E. Tennant, C.A. Cockrum, J.B. Gilpin, M.A. Kinch, M.B. Reine and R.P. Ruth, *Journal of Vacuum Science Technology*, B 10(4), pp. 1359-1369, Jul/Aug 1992.
2. J.B. Mullin, *SPIE Vol. 1512 Infrared and Optoelectronic Materials and Devices*, pp. 144-154, 1991.
3. S. Sen, W.H. Konkel, S.J. Tighe, L.G. Bland, S.R. Sharma and R.E. Taylor, *J. Crystal Growth*, 86, pp. 111-117, 1988.
4. S. McDevitt, D.R. John, J.L. Sepich, K.A. Bowers, J.F. Schetzina, R.S. Rai, and S. Mahajan, *Materials Research Society Symposium Proceedings*, Vol. 161, pp. 15-26, 1990.
5. P. Rudolph and M. Muhlberg, *Materials Science and Engineering*, B16, pp. 8-16, 1993.
6. M. Pfeiffer and M. Muhlberg, *J. Crystal Growth*, 118, pp. 269-276, 1992.
7. P. Brunet, A. Katty, D. Schneider, A. Tromson-Carli, and R. Triboulet, *Materials Science and Engineering*, B16, pp. 44-47, 1993.
8. H.N.G. Wadley and B.W. Choi, *J. Crystal Growth*, in press, 1996.
9. K.P. Dharmasena and H.N.G. Wadley, "Eddy current sensor concepts for the Bridgman growth of semiconductors", *J. Crystal Growth*, in press, 1996.
10. K.P. Dharmasena and H.N.G. Wadley, *Review of Progress in Quantitative Nondestructive Evaluation*, Eds. D.O. Thompson and D.E. Chimenti, Plenum Press, New York, Vol. 15, pp. 2241-2248, 1996.
11. K.P. Dharmasena and H.N.G. Wadley, "Eddy current sensing of vertical Bridgman growth of  $\text{Cd}_{0.96}\text{Zn}_{0.04}\text{Te}$ ", *J. Crystal Growth*, in press, 1996.
12. K.P. Dharmasena and H.N.G. Wadley, *Rev. Sci. Instrum.*, accepted for publication, 1996.